Spectroscopy of AuO: Identification of the [10.7] $\Pi_{3/2}$ to $X^2\Pi_{3/2}$ Transition

Leah C. O'Brien,*,† Sarah C. Hardimon,† and James J. O'Brien‡

Department of Chemistry, Southern Illinois University−Edwardsville, Edwardsville, Illinois 62026-1652, and Department of Chemistry and Biochemistry, University of Missouri−St. Louis, St. Louis, Missouri 63121-4499

Received: September 15, 2004; In Final Form: October 13, 2004

The near-infrared electronic spectrum of AuO has been recorded in emission using the Fourier transform spectrometer associated with the National Solar Observatory at Kitt Peak, AZ. The gas-phase AuO molecules were produced in a neon-based electric discharge using a gold-lined hollow cathode with a trace amount of oxygen. Two bands observed in the spectrum, with red-degraded bandheads located at 10665 and 10726 cm^{-1}, are assigned as the (1,1) and (0,0) bands of the $\Pi_{3/2}$ to $X^2\Pi_{3/2}$ transition, respectively. Results of the analysis are presented. This work and the accompanying paper[1] on the photoelectron spectrum of AuO and AuO^- represent the first spectral observations of gas-phase AuO.

Introduction

In our laboratory, we have studied electronic transitions of the coinage metal oxides (CuO[2] and AgO[3,4]), a sulfide (CuS[5]), and a selenide (CuSe[6]). The comparison of gold to other coinage metal oxides reveals trends in bonding for the group 11 metals and illustrates the strong relativistic effects in gold.

Gas phase gold oxide, AuO, has not been observed previously by any spectroscopic method, and little else is known or predicted about gold oxide. Griffiths and Barrow[7] recorded the UV/visible spectrum of AuO in rare gas matrixes and observed an electronic transition at approximately 25 000 cm^{-1}. Hecq et al.[8] determined the Au−O bond energy to be about 3 eV by glow discharge mass spectrometry. More recently, Schwerdtfeger et al.[9] used nonrelativistic and relativistic Hartree−Fock and configuration interaction calculations to predict a number of spectroscopic properties, such as bond lengths, dissociation energies, force constants, and dipole moments for the $X^2\Pi$ and $A^2\Sigma$ states of AuO. Using the B3PW91/LANL-2DZ and -E levels of theory, Seminario et al.[10] calculated the bond length for AuO to be 1.925 Å.

This work and the accompanying paper[1] represent the first spectral observations of gas-phase AuO.

Materials and Methods

The near-infrared spectrum of AuO has been recorded in emission using the Fourier transform spectrometer associated with the McMath-Pierce National Solar Observatory at Kitt Peak, AZ. The gas phase AuO molecules were produced in a neon-based electric discharge using a gold-lined hollow cathode and a trace amount of oxygen. The neon partial pressure was 2.8 Torr, and the oxygen pressure was approximately 20 mTorr. The discharge operated at 430 mA with an applied potential of 430 V. The FT spectrometer was configured with a CaF_2 beam splitter, GaAs filter, and liquid-nitrogen cooled InSb detectors, to record in the 3500−12 000 cm^{-1} region. The resolution was set at 0.020 cm^{-1}, and the total integration time was 150 min.

* Corresponding author. E-mail: lobrien@siue.edu.
† Southern Illinois University−Edwardsville.
‡ University of Missouri−St. Louis.

Results and Discussion

Two red-degraded bands were observed in the spectrum with bandheads located at 10 665 and 10 726 cm^{-1}. The 10 726 cm^{-1} band is approximately 50% more intense than the 10 665 cm^{-1} band. Two R-type branches and two P-type branches were observed in each band. To determine line positions, the identified lines were fit to a Voigt profile using the program *GREMLIN*, written by James Brault (formerly of National Solar Observatory−Kitt Peak). A portion of the $^{197}Au^{16}O$ spectrum is shown in Figure 1. Lack of any observable structure due to isotopomers helps confirm the assignment of these transitions to AuO since ^{197}Au is 100% abundant. The line width of an isolated, unblended line is approximately 0.028 cm^{-1}, indicating that the linewdith is primarily Doppler-limited. The line width does not appear to be *J* dependent.

Predictions of ground-state symmetry and molecular parameters were important to the assignment of the spectrum. Schwerdtfeger et al.[9] predicted the ground-state symmetry of AuO to be $X^2\Pi_i$. To obtain a rough estimate of the ground-state spin−orbit splitting, we performed a Fenske−Hall type calculation[11] for AuO using the r_e value of 1.9 Å from Schwerdtfeger et al.[9] and Seminario et al.[10] A modified molecular orbital (MO) energy level diagram of the valence orbitals determined from our calculation is shown in Figure 2, where the position along the *x*-axis indicates the % oxygen character. As shown in the MO diagram, the ground-state valence electron configuration is predicted to be $15\sigma^2 8\pi^4 4\delta^4 16\sigma^2 9\pi^3$, arising primarily from the atomic configuration $Au^+[5d^{10}]O^-[2p\sigma^2 2p\pi^3]$. Although the Fenske−Hall type calculation is not quantitative, the MO diagram gives a reasonable representation of the ground state electronic structure. Clearly, the spin−orbit splitting will arise from the electron hole in a 9π orbital. From our calculation, the 9π orbital has approximately 80% oxygen 2p character and 20% gold 3d character. Using the atomic spin−orbit splittings,[12] we estimated the ground-state spin−orbit splitting to be $A_{SO} = -1000$ cm^{-1}. Our low-level calculation supports the ab initio and experimental work given in the companion paper,[1] where they found $A_{SO}(\text{expt}) = -1440 \pm 80$ cm^{-1}.

On the basis of our previous work on the isovalent molecules CuO, CuS, CuSe, and AgO,[2−6] we anticipated a $^2\Sigma^+$ to $X^2\Pi_i$

10.1021/jp045812m CCC: $27.50
Published on Web 11/26/2004

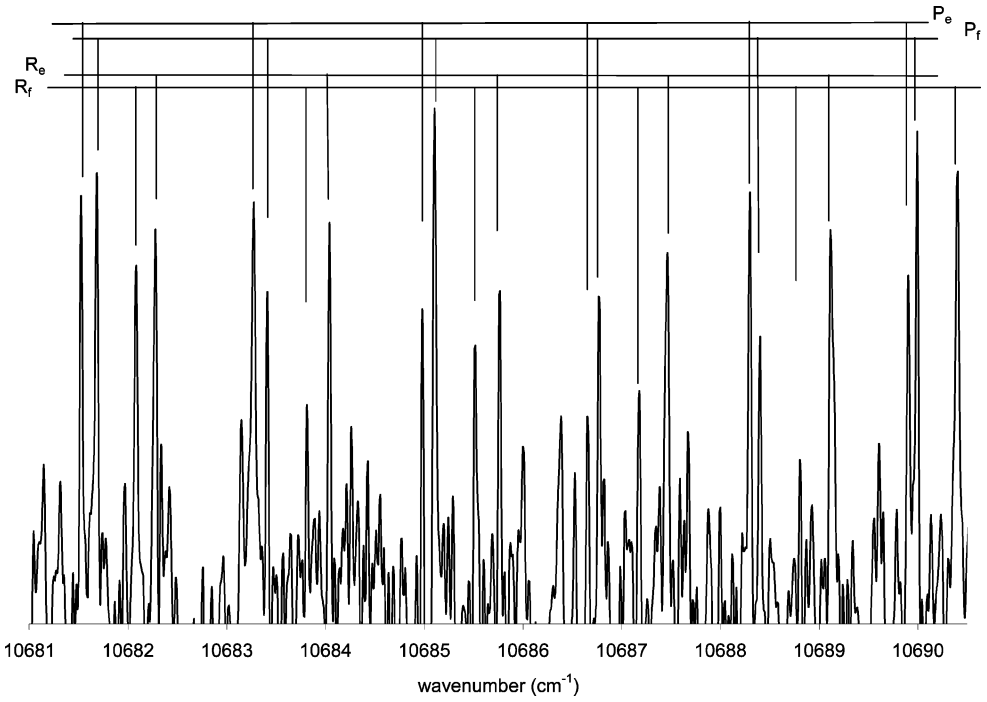

Figure 1. Portion of the AuO spectrum showing the (0,0) band of the $\Pi_{3/2}$ to $X^2\Pi_{3/2}$ transition.

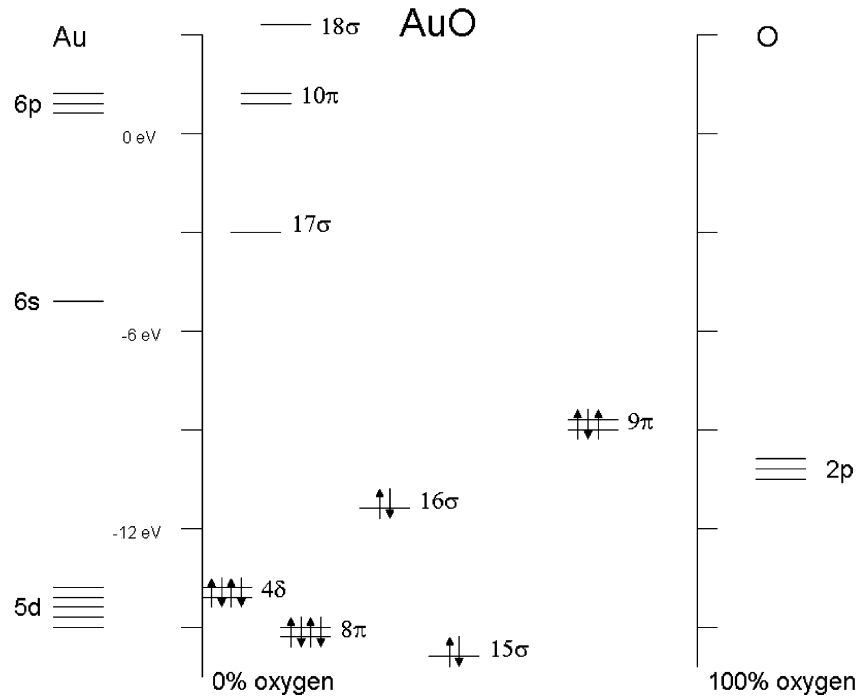

Figure 2. Modified molecular orbital energy level diagram for AuO, where the position of the orbital along the *x*-axis indicates the % oxygen character.

transition in the near-infrared. This transition occurs by excitation of a 16σ electron to the 9π orbital, resulting in the low-lying $A\ ^2\Sigma^+$ state.[2−6] However, having observed only two P-branches and two R-branches for each band, this was clearly not the case. The two strongest branches in each band of the $^2\Sigma^+$ to $X^2\Pi_i$ spectra are both Q-branches, but no Q-branches were observed in our spectrum. Additionally, our estimated spin−orbit splitting in the $X^2\Pi$ state (A_{SO}= −1000 cm^{-1}) eliminated the possibility that the observed bands were the $^2\Sigma^+$ to $X^2\Pi_{3/2}$ and $^2\Sigma^+$ to $X^2\Pi_{1/2}$ transitions since the spacing between the observed bandheads was only 61 cm^{-1}. Possible assignments consistent with the observed branches were $^2\Sigma^+$ to $^2\Sigma^+$ transitions or subbands of $^{2,4}\Pi$ to $^2\Pi$ transitions. Since the ground state symmetry is most certainly $X^2\Pi_{3/2}$, we favored the latter assignment. Indeed, both bands could be fit as $^2\Pi_{3/2}$ to $^2\Pi_{3/2}$ transitions, from which we conclude that the 10 726 and 10 665 cm^{-1} bands are the (0,0) and (1,1) bands, respectively, of a new [10.7] $\Pi_{3/2}$ to $X^2\Pi_{3/2}$ transition, where the value in brackets identifies the term value of the excited state in units of 1000 cm^{-1}. A search for low-*J* Q lines proved unsuccessful, as this region is obscured by strong R lines returning from the bandhead.

The spin multiplicity of the excited state cannot be determined from the analysis; thus, a multiplicity is not given. Ichino et

TABLE 1: Line Positions, Assignments, and Residuals for the (0,0) Band of the [10.7] $\Pi_{3/2}$ to $X^2\Pi_{3/2}$ Transition of AuO (in cm^{-1})

J''	Pe(J'')	$o-c$	Pf(J'')	$o-c$	Re(J'')	$o-c$	Rf(J'')	$o-c$
11.5	10711.905	0.005	10711.905	0.001				
12.5	10710.881	0.000	10710.881	−0.006				
13.5	10709.835	0.007	10709.835	−0.001				
14.5	10708.749	0.008	10708.749	−0.002				
15.5	10707.631	0.012	10707.631	−0.001				
16.5	10706.472	0.009	10706.472	−0.006				
17.5	10705.279	0.007	10705.299	0.008				
18.5	10704.057	0.010	10704.071	0.001	10726.401	0.008		
19.5	10702.786	−0.002	10702.818	0.004	10726.311	0.005		
20.5	10701.493	−0.001	10701.516	−0.009	10726.189	0.005		
21.5	10700.169	0.004	10700.201	−0.001	10726.028	0.000	10726.094	0.002
22.5	10698.800	−0.002	10698.852	0.007	10725.837	0.001	10725.903	−0.006
23.5	10697.398	−0.006	10697.457	0.003	10725.610	0.000	10725.690	−0.002
24.5	10695.972	0.000	10696.026	−0.003	10725.348	0.000	10725.442	0.002
25.5	10694.509	0.003	10694.570	0.000	10725.051	−0.001	10725.148	−0.006
26.5	10693.002	−0.003	10693.081	0.004	10724.722	0.002	10724.836	0.002
27.5	10691.472	0.003	10691.552	0.001	10724.355	0.002	10724.478	−0.001
28.5	10689.904	0.005	10689.990	−0.001	10723.957	0.006	10724.086	−0.004
29.5	10688.297	0.003	10688.400	0.004	10723.516	0.002	10723.672	0.005
30.5	10686.655	0.000	10686.772	0.004	10723.034	−0.007	10723.206	−0.003
31.5	10684.981	0.000	10685.107	0.000	10722.535	0.002	10722.712	−0.005
32.5	10683.268	−0.004	10683.410	−0.001	10721.988	−0.002	10722.188	−0.003
33.5	10681.526	−0.003	10681.680	−0.002	10721.418	0.006	10721.627	−0.003
34.5	10679.749	−0.002	10679.921	0.002	10720.801	0.003	10721.033	−0.002
35.5	10677.942	0.004	10678.119	−0.003	10720.143	−0.006	10720.406	0.000
36.5	10676.091	0.000	10676.289	−0.003	10719.467	0.003	10719.742	0.000
37.5	10674.213	0.004	10674.428	0.000	10718.744	0.000	10719.041	−0.003
38.5	10672.293	0.000	10672.526	−0.004	10717.989	0.000	10718.309	−0.002
39.5	10670.341	0.000	10670.597	−0.001	10717.198	0.000	10717.547	0.003
40.5	10668.356	0.001	10668.631	−0.002	10716.371	0.000	10716.743	0.000
41.5	10666.333	−0.002	10666.637	0.002	10715.508	−0.001	10715.906	−0.002
42.5	10664.283	0.004	10664.606	0.004	10714.610	−0.001	10715.033	−0.005
43.5	10662.187	−0.002	10662.530	−0.006	10713.673	−0.004	10714.130	−0.003
44.5	10660.065	0.001	10660.428	−0.009	10712.707	−0.001	10713.189	−0.005
45.5	10657.897	−0.007	10658.308	0.005	10711.705	0.002	10712.222	0.001
46.5	10655.710	0.001	10656.141	0.004	10710.666	0.004	10711.207	−0.006
47.5	10653.483	0.003	10653.929	−0.007	10709.580	−0.005	10710.171	0.000
48.5	10651.214	−0.002	10651.699	−0.003	10708.470	−0.003	10709.094	−0.001
49.5	10648.918	0.002	10649.430	−0.005	10707.328	0.004	10707.984	0.000
50.5	10646.588	0.006	10647.119	−0.015	10706.137	−0.003	10706.837	−0.001
51.5	10644.209	−0.004	10644.806	0.006	10704.921	0.001	10705.655	−0.003
52.5	10641.809	0.000	10642.433	0.001	10703.667	0.004	10704.443	−0.001
53.5	10639.375	0.005	10640.028	−0.002	10702.373	0.002	10703.194	−0.001
54.5	10636.899	0.003	10637.590	−0.005	10701.044	0.001	10701.910	−0.001
55.5	10634.389	0.001	10635.124	−0.002	10699.682	0.004	10700.592	−0.001
56.5	10631.847	0.003	10632.624	0.000	10698.280	0.003	10699.245	0.005
57.5	10629.267	0.002	10630.082	−0.007	10696.839	−0.001	10697.856	0.003
58.5	10626.646	−0.005	10627.516	−0.004	10695.365	−0.002	10696.431	−0.001
59.5	10624.003	0.001	10624.924	0.006	10693.868	0.010	10694.975	−0.001
60.5	10621.312	−0.006	10622.284	0.002	10692.313	0.001	10693.489	0.004
61.5	10618.599	0.000	10619.618	0.005	10690.733	0.003	10691.968	0.009
62.5	10615.847	0.003	10616.906	−0.004	10689.116	0.005	10690.398	−0.001
63.5	10613.054	−0.001	10614.181	0.007	10687.456	0.000	10688.807	0.002
64.5	10610.231	0.001	10611.411	0.007	10685.764	−0.001	10687.175	−0.001
65.5	10607.376	0.005	10608.601	0.000	10684.041	0.005	10685.517	0.005
66.5	10604.480	0.004	10605.771	0.006	10682.275	0.003	10683.814	0.001
67.5	10601.544	−0.001	10602.894	−0.001	10680.473	0.002	10682.081	0.001
68.5	10598.583	0.003	10599.983	−0.009	10678.634	0.001	10680.310	−0.002
69.5	10595.578	−0.001	10597.054	−0.001	10676.752	−0.006	10678.508	−0.002
70.5	10592.547	0.004	10594.081	−0.004	10674.845	−0.002	10676.673	0.001
71.5	10589.471	0.000	10591.078	−0.004	10672.897	−0.002	10674.801	0.001
72.5	10586.364	−0.001	10588.049	0.004	10670.910	−0.004	10672.897	0.003
73.5	10583.213	−0.009	10584.980	0.005	10668.885	−0.007	10670.952	0.000
74.5	10580.041	−0.004	10581.873	0.001			10668.969	−0.007

al.[1] have used high level ab initio calculations to predict excited-state term energies. They have found the first $^2\Pi$ to $X^2\Pi$ transition to be around 3 eV for AuO and the first $^4\Pi$ to $X^2\Pi$ transition to be near 2.1 eV. The $^2\Pi$ to $X^2\Pi$ transition energy predicted by Ichino et al.[1] well matches the UV−vis absorption attributed to AuO in rare gas matrixes by Griffiths and Barrow.[7] Our transition could be the $^4\Pi_{3/2}$ to $X^2\Pi_{3/2}$ transition, which becomes allowed through doublet-quartet mixing by the spin−orbit interaction. Perhaps as more work on AuO is recorded and analyzed, a clearer picture of the general electronic structure will be revealed.

Since only one spin−orbit component of each Π state was observed, the standard 2×2 Hamiltonian for a Hund's case $(a)^2\Pi$ state could not be used. A simple polynomial expression

TABLE 2: Line Positions, Assignments, and Residuals for the (1,1) Band of the [10.7] $\Pi_{3/2}$ to $X^2\Pi_{3/2}$ Transition of AuO (in cm^{-1})

J''	Pf(J'')	$o-c$	Pe(J'')	$o-c$	Rf(J'')	$o-c$	Re(J'')	$o-c$
8.5	10653.110	−0.001	10653.109	−0.001				
9.5	10652.196	0.000	10652.212	0.018				
10.5	10651.246	−0.001	10651.259	0.016				
11.5	10650.272	0.010	10650.272	0.014				
12.5	10649.253	0.011	10649.253	0.017				
13.5	10648.195	0.007	10648.195	0.015				
14.5	10647.098	0.000	10647.088	0.000				
15.5	10645.977	0.003	10645.968	0.007				
16.5	10644.812	−0.002	10644.798	−0.001				
17.5	10643.614	−0.006	10643.593	−0.009				
18.5	10642.386	−0.005	10642.368	−0.001				
19.5	10641.121	−0.006	10641.096	−0.004	10664.355	0.000		
20.5	10639.822	−0.006	10639.797	0.000	10664.218	0.003	10664.161	0.003
21.5	10638.500	0.005	10638.460	0.002	10664.035	−0.005	10663.978	0.002
22.5	10637.134	0.008	10637.081	−0.003	10663.829	−0.001	10663.760	0.003
23.5	10635.722	−0.001	10635.673	−0.001	10663.577	−0.007	10663.509	0.006
24.5	10634.288	0.003	10634.229	0.000	10663.302	−0.002	10663.211	−0.001
25.5	10632.815	0.003	10632.749	0.001	10662.993	0.005	10662.879	−0.007
26.5	10631.307	0.002	10631.232	−0.001	10662.634	−0.003	10662.524	0.001
27.5	10629.770	0.008	10629.680	−0.001	10662.250	0.000	10662.124	−0.001
28.5	10628.191	0.006	10628.096	0.002	10661.826	−0.003	10661.689	−0.001
29.5	10626.576	0.002	10626.475	0.003	10661.368	−0.004	10661.214	−0.005
30.5	10624.926	−0.001	10624.820	0.006	10660.876	−0.004	10660.716	0.004
31.5	10623.244	−0.002	10623.122	0.001	10660.350	−0.002	10660.166	−0.003
32.5	10621.527	−0.003	10621.389	−0.003	10659.789	−0.001	10659.594	0.004
33.5	10619.781	0.002	10619.621	−0.006	10659.194	0.002	10658.976	0.002
34.5	10617.993	−0.001	10617.827	0.000	10658.553	−0.005	10658.312	−0.010
35.5	10616.176	0.002	10615.993	0.001	10657.897	0.007	10657.637	0.003
36.5	10614.322	0.002	10614.119	−0.001	10657.179	−0.007	10656.905	−0.004
37.5	10612.428	−0.002	10612.216	0.003	10656.447	0.001	10656.149	0.002
38.5	10610.505	−0.001	10610.267	−0.004	10655.668	−0.003	10655.351	0.001
39.5	10608.548	0.000	10608.293	0.000	10654.856	−0.005	10654.519	0.004
40.5	10606.545	−0.010	10606.273	−0.006	10654.009	−0.007	10653.644	0.000
41.5	10604.530	0.003	10604.227	−0.002	10653.122	−0.013	10652.738	0.001
42.5	10602.467	0.003	10602.141	−0.002	10652.212	−0.006	10651.788	−0.004
43.5	10600.364	−0.003	10600.021	−0.001	10651.262	−0.004	10650.810	−0.001
44.5	10598.222	−0.013	10597.858	−0.007	10650.278	−0.001	10649.788	−0.006
45.5	10596.061	−0.008	10595.672	0.000	10649.259	0.003	10648.737	−0.002
46.5	10593.872	0.004	10593.440	−0.003	10648.195	−0.002	10647.645	−0.003
47.5	10591.631	−0.001	10591.179	0.001	10647.119	0.016	10646.524	0.005
48.5	10589.359	−0.003	10588.873	−0.005	10645.974	0.000	10645.356	0.002
49.5	10587.053	−0.004	10586.541	0.000	10644.807	−0.002	10644.154	0.003
50.5	10584.723	0.006	10584.169	0.001	10643.605	−0.003	10642.918	0.006
51.5	10582.338	−0.005	10581.760	0.000	10642.378	0.006	10641.636	0.001
52.5	10579.930	−0.004	10579.319	0.004	10641.103	0.003	10640.322	0.000
53.5	10577.485	−0.005	10576.831	−0.004	10639.799	0.007	10638.971	0.000
54.5	10575.005	−0.007	10574.320	0.002	10638.443	−0.005	10637.582	−0.001
55.5	10572.506	0.007	10571.768	0.003	10637.081	0.012	10636.154	−0.003
56.5	10569.954	0.002	10569.175	−0.001	10635.653	−0.002	10634.689	−0.005
57.5	10567.367	−0.003	10566.554	0.003	10634.214	0.010	10633.190	−0.004
58.5	10564.757	0.004	10563.888	−0.001	10632.720	0.002	10631.656	0.000
59.5	10562.106	0.004	10561.192	0.001	10631.190	−0.006	10630.088	0.007
60.5	10559.412	−0.004	10558.463	0.006	10629.642	0.004	10628.468	0.000
61.5	10556.700	0.005	10555.687	0.000	10628.045	0.001	10626.824	0.006
62.5	10553.942	0.002	10552.877	−0.003	10626.421	0.007	10625.132	0.003
63.5	10551.149	−0.001	10550.039	0.002	10624.743	−0.005	10623.404	0.000
64.5					10623.049	0.002	10621.641	0.001
65.5					10621.309	0.000	10619.833	−0.005
66.5					10619.538	0.003	10617.993	−0.006
67.5					10617.727	0.001	10616.124	0.003
68.5					10615.884	0.004		
69.5					10613.996	−0.002		
70.5					10612.076	−0.004		

for the $^2\Pi_{3/2}$ energy levels[13] was used in the nonlinear least-squares fit where the upper/lower sign is used for the e/f level:

$$T = T_v + B_v J(J+1) - D_v J^2(J+1)^2 \pm 0.5 q_J J(J+1)(J+0.5) \quad (1)$$

A total of 458 lines included in the fit gave an average residual of the unblended lines of <0.004 cm^{-1}, which is consistent with the experimental uncertainty. Line positions, assignments, and fit residuals are presented in Tables 1 and 2. The molecular parameters determined by the fit are given in Table 3.

The molecular parameters are consistent with the assignment of the two observed bands as a short vibrational sequence. As expected, the rotational constants of the $v = 1$ levels, $B_{1'}$ and

TABLE 3: Molecular Parameters for the $X^2\Pi_{3/2}$ and [10.7] $\Pi_{3/2}$ States of AuO (in cm^{-1})[a]

	T_v	B_v	$D_v \times 10^6$	$q_{Jv} \times 10^5$
[10.7] $\Pi_{3/2}$ $v = 1$	$\Delta G_{1/2} + 10659.4694(10)$	0.2905442(88)	0.4275(15)	−0.9451(82)
[10.7] $\Pi_{3/2}$ $v = 0$	10721.1415(8)	0.2944496(63)	0.41145(84)	−0.9358(55)
$X^2\Pi_{3/2}$ $v = 1$	$\Delta G_{1/2} \approx 590(70)$[b]	0.3081398(91)	0.4068(16)	−0.4771(83)
$X^2\Pi_{3/2}$ $v = 0$	0.0	0.3116286(63)	0.39998(84)	−0.4658(55)

[a] Values in parentheses represent 1 σ error. [b] From ref 1.

$B_{1''}$, are slightly smaller than the rotational constants of the $v = 0$ levels, $B_{0'}$ and $B_{0''}$, due to the slight increase in bond length based on an anharmonic oscillator potential. Additionally, the assignment of the spectrum to the (0,0) and (1,1) bands is consistent with the observed relative intensity of the two bands, where the 10 726 cm^{-1} band is approximately 50% more intense than the 10 665 cm^{-1} band. It is clear that the 10 665 cm^{-1} band is a hot band of the 10 726 cm^{-1} band. It should be noted, however, that the absolute vibrational assignment is not definitive from this observation. For example, the bands could be the (0,1) and (1,2) bands or the (1,0) and (2,1) bands. The matrix work of Griffith and Barrow[7] did not record the near-infrared region and thus adds no insight to the absolute vibrational assignments. However, it has been our experience that emission from $v' = 0$ is the most intense for the many related transition-metal containing diatomics that we have observed.[2−6] Thus, the primary evidence for the vibrational assignments comes from the lack of bands appearing elsewhere in the frequency region that was recorded (3500−12 000 cm^{-1}), and we do feel confident in our assignment of the bands as (0,0) and (1,1) transitions.

The rotational constants determined from the fit can be used to determine the Dunham-type coefficients and bond lengths. For the ground $X^2\Pi_{3/2}$ state, $B_e = 0.3133730(78)$ cm^{-1}, $\alpha_e = 0.0034888(78)$ cm^{-1}, $r_0 = 1.9122$ Å, and $r_1 = 1.9230$ Å, from which we can extrapolate $r_e = 1.9069$ Å. This is in reasonable agreement with the ground state ab initio results of $r_e = 1.946$ and 1.925 Å by Schwerdtfeger et al.[9] and Seminario et al.,[10] respectively, and in excellent agreement with the ab initio result from Ichino et al.,[1] $r_e = 1.907$ Å. For the excited $\Pi_{3/2}$ state, $B_e = 0.2964023(77)$ cm^{-1}, $\alpha_e = 0.0039054(77)$ cm^{-1}, $r_0 = 1.9672$ Å, and $r_1 = 1.9804$ Å, from which we can extrapolate $r_e = 1.9607$ Å.

Schwerdtfeger et al.[9] predicted a low-lying $^2\Sigma^+$ state at 10 800 cm^{-1}. With this information, the unique perturber relationship can be used to estimate the lambda-doubling parameter for the $X^2\Pi_{3/2}$ state using $l = 1$ for the valence p-orbitals:[12]

$$q_J = 2B^2 l(l+1)/(E_\Pi - E_\Sigma) = -3.6 \times 10^{-5}\ \text{cm}^{-1} \quad (2)$$

The e/f symmetry components of the lambda doublets were assigned such that q_J of the $X^2\Pi_{3/2}$ state would be negative. It should be noted that this assignment is not certain given the inherent errors of the unique perturber approximation.[12] The magnitude of the predicted value is about 1 order of magnitude larger than the observed value for the ground state, $q_J = -0.4658(55) \times 10^{-5}$ cm^{-1}.

The vibrational frequencies for the electronic states could not be determined directly from the fit because the identified (0,0) and (1,1) bands do not have a common state. However, the difference in band origins between the two bands is determined from the analysis to be 62 cm^{-1}. This difference represents the change in vibrational interval between the [10.7] $\Pi_{3/2}$ state and the $X^2\Pi_{3/2}$ state. Ichino et al.[1] determined the vibrational interval of the $X^2\Pi_{1/2}$ state to be $\Delta G_{1/2} = 590 \pm 70$ cm^{-1}, and this is also a reasonable estimate for the vibrational interval of the $X^2\Pi_{3/2}$ state. Thus, the vibrational interval for the [10.7] $\Pi_{3/2}$ state is estimated to be $\Delta G_{1/2} = 528 \pm 70$ cm^{-1}.

The bond lengths in the ground states of CuO, AgO, and AuO highlight the relativistic effects in the Au atom: r_0(CuO) = 1.791 Å, r_0(AgO) = 2.077 Å, and r_0(AuO) = 1.912 Å. The lanthanide contraction is well-known and useful in explaining much of the decrease in bond length expected for AuO: the valence electrons are pulled inward due to the increase in effective nuclear charge from the poor shielding effect of the f-electrons.[14] However, direct relativistic effects[9] also must be included to accurately predict molecular properties such as bond lengths: the closest predictions have resulted from relativistic calculations.[1,9,10]

Acknowledgment. Support for this work was provided by the National Science Foundation. The authors thank Mike Dulick, Scott Rixon, Jim Peers, and Chris Kingston for their help with the experimental setup and data collection. The authors thank Carl Lineberger and Takatoshi Ichino for useful discussions and sharing the data on the photoelectron spectrum of AuO/AuO$^-$.

References and Notes

(1) Ichino, T.; Gianola, A. J.; Andrews, D. H.; Lineberger, W. C. Photoelectron spectroscopy of AuO$^-$ and AuS$^-$. *J. Phys. Chem. A* **2004,** 11307.

(2) O'Brien, L. C.; Kubicek, R. L.; Koch, D. L.; Wall, S. J.; Friend, R.; Brazier, C. R. *J. Mol. Spectrosc.* **1996**, *180*, 365−368.

(3) O'Brien, L. C.; Wall, S. J.; Sieber, M. K. *J. Mol. Spectrosc.* **1997**, *183*, 57−60.

(4) O'Brien, L. C.; Wall, S. J.; Henry, G. L. *J. Mol. Spectrosc.* **1998**, *191*, 218−220.

(5) O'Brien, L. C.; Dulick, M.; Davis, S. P. *J. Mol. Spectrosc.* **1999**, *195*, 328−331.

(6) O'Brien, L. C.; Lambeth, A. K.; Brazier, C. R. *J. Mol. Spectrosc.* **2002**, *213*, 64−68.

(7) Griffiths, M. J.; Barrow, R. F. *J. Chem. Soc., Faraday Trans. 2* **1977**, *73*, 943−947.

(8) Hecq, A.; Vandy, M.; Hecq, M. *J. Chem. Phys.* **1980**, *72*, 2876−1879.

(9) Schwerdtfeger, P.; Dolg, M.; Schwarz, W. H. E.; Bowmaker, G. A.; Boyd, P. D. W. *J. Chem. Phys.* **1989**, *91*, 1762−1774.

(10) Seminario, J. M.; Zacarias, A. G.; Tour, J. M. *J. Am. Chem. Soc.* **1999**, *121*, 411−416.

(11) Hall, M. B.; Fenske, R. F. *Inorg. Chem.* **1972**, *11*, 768−775.

(12) Lefebvre-Brion, H.; Field, R. W. *Perturbations in the Spectra of Diatomic Molecules*; Academic Press: New York, 1986.

(13) Hirao, T.; Dufour, C.; Pinchemel, B.; Bernath, P. F. *J. Mol. Spectrosc.* **2000**, *202*, 53−58.

(14) Jones, L. L.; Atkins, P. W. *Chemistry—Molecules, Matter and Change*; W. H. Freeman Press: New York, 2000.